CONF-871243--1

UCRL- 97722
PREPRINT

PROMPT PROCESSES IN HEAVY ION REACTIONS

Marshall Blann
Bruce A. Remington

This paper was prepared for submittal to
Texas A&M Symposium on Hot Nuclei
College Station, Texas
December 7-10, 1987

December 1987

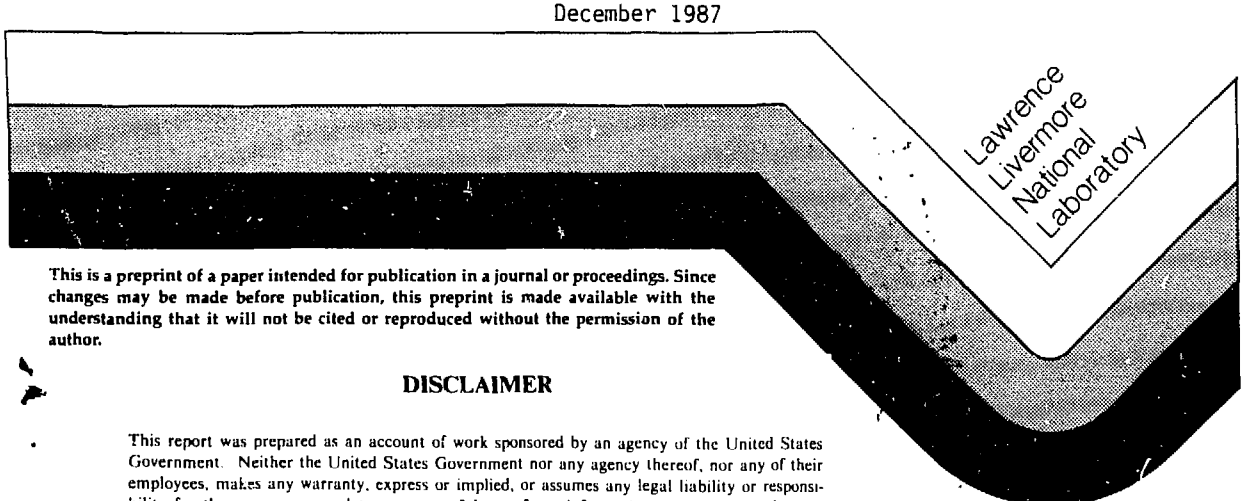

PROMPT PROCESSES IN HEAVY ION REACTIONS

Marshall Blann and Bruce A. Remington
E-Division, Physics Department
University of California
Lawrence Livermore National Laboratory
Livermore, California U.S.A.

UCRL--97722

DE88 004399

ABSTRACT: We test a relaxation model based on two body nucleon-nucleon scattering processes to interpret phenomena observed in heavy ion reactions. We use the Boltzmann Master Equation to accomplish this. By assuming that the projectile nucleons partition the total excitation with equal a-priori probability of all configurations, we are able to reproduce several sets of neutron spectra from ^{20}Ne and ^{12}C induced reactions on ^{165}Ho and from reactions of ^{40}Ar or ^{40}Ca. We point out ambiguities in deducing angle-integrated energy spectra from double differential spectra. With no additional free parameters, our model successfully reproduces a large body of high energy γ-ray spectra by assuming an incoherent n-p-bremsstrahlung mechanism.

1.0 INTRODUCTION

As heavy ion reaction studies progressed from beam energies below 10 MeV/nucleon into the medium energy range, many non-equilibrium reaction phenomena have been observed. Nucleons are emitted with velocities far in excess of the beam velocity and with cross sections orders of magnitude above the equilibrium expectation.[1-3] Pion emission has been observed at beam energies per nucleon which are much less than the free N-N-π threshold energy.[4-7] Gamma-rays in excess of 100 MeV have been observed at projectile energies as low as 20 to 30 MeV per nucleon.[8-14]

The intriguing question is how so much of the total energy available in the reaction entrance channel becomes focused on a

single entity in the exit channel? We try to understand and interpret these phenomena in terms of nuclear models or nuclear theories.

One fascinating and quite successful approach is due to Greiner and his colleagues,[15] and is based on a collective bremsstrahlung resulting from the slowing down of target and projectile nuclei (in the center-of-mass frame) as the nuclear densities start to overlap. Many other approaches rely on a mechanism due to incoherent nucleon-nucleon (N-N) scattering processes in the mean nuclear field.[16-24] In this presentation, we would like to attempt an explanation of all these phenomena in a very physically transparent model of the latter type. The numerical approach we will take will be the Boltzmann Master Equation (BME), originally applied to nucleon induced reactions by Harp et al.[25,26]

We shall first describe the physical model we use and the mathematical method of computer solution. Next, we will test the one parameter of the model which we guess (based on earlier precompound studies with alpha particles) by comparing with experimental (HI,n) spectra. Next, we will consider the question of the fundamental NNγ bremsstrahlung cross sections as a function of energy. The above two results are then used without further adjustment to reproduce absolute nucleon-nucleus and nucleus-nucleus γ-ray spectra, with no free parameters. Finally, we will present our conclusion as to whether or not the incoherent N-N collision mechanism is one of the viable explanations for these many non-equilibrium phenomena.

2.0 PHYSICS AND FORMULATION OF THE BOLTZMANN MASTER EQUATION

In Fig. 1, we see a diagrammatic representation of the reaction of two heavy ions. In the upper portion of the figure we see two nuclei approaching one another in a geometric representation. The nuclei each have a spherical shape, with the nucleons bound inside each nucleus by the surface tension. Once the two nuclei touch, the interface disappears, and the surface tension and beam momentum combine in driving the system towards coalescence.

In the lower portion of Fig. 1, we represent the same reaction in an energy space represented by the bound potential wells of the two nuclei. The formation of the neck described in the geometric picture means that the nucleons of target and projectile may now begin to interact in a time dependent manner in some joint potential well formed in the coalescence process. This energy space is the representation used in the BME.

The mathematical approach used in solving this problem is partly defined in Fig. 2, where we clarify the indexing used in the potential of the coalesced nuclear system. The model is based on nucleon-nucleon (N-N) collisions using free N-N scattering cross sections to define collision rates ω_{kl}, where

$$\omega^{xy}_{kl\to ij} = \frac{\sigma_{kl}[(2/m)(\varepsilon_k+\varepsilon_l)]^{1/2}}{V \sum'_{q,p} g_q g_p} \qquad (1)$$

Here, V is the nuclear volume and σ_{kl} is the free nucleon-nucleon scattering cross section for the nucleons of energy k+l. The master equations are given by:

$$\frac{dN^x_i}{dt} = g^x_i \sum_y \sum'_{jkl} [\omega^{xy}_{kl\to ij} g^x_k g^y_l g^y_j n^x_k n^y_l (1-n^x_i)(1-n^y_j) - \omega^{xy}_{ij\to kl} g^y_j g^x_k g^y_l n^x_i n^y_j (1-n^x_k)(1-n^y_l)] \qquad (2)$$

$$- n^x_i \omega^x_{i\to i'} + f^x_i(t) \quad ,$$

the prime on the summation sign indicating that the summations are conducted respecting energy conservation. The superscripts x,y differentiate neutrons from protons in a two-component Fermi gas, and the subscripts i,j,k,l denote the energies of 1-MeV-wide bins above the bottom of the nuclear well. The g^x_i give the density of single-particle states at energy i for nucleons of type x, as calculated in the Fermi gas model. The n^x_i denote the fraction of

levels in the 1 MeV-wide bin at energy i which are occupied by a nucleon of type x, and the Pauli exclusion principle is embodied in the $1-n_i^x$ factors. The $\omega^{xy}_{kl\rightarrow ij}$ represent the rate at which a nucleon of type x at energy k scatters from a nucleon of type y at energy l to give nucleons at energies i and j. The $f_i^x(t)$ term is a source term, representing a time dependent injection of nucleons of type x and excitation energy during the coalescence (fusion) process; this term will be discussed shortly. A more thorough discussion of the BME, as encoded originally by Harp, Miller, and Berne, and later modified by Blann, may be found in Refs. 16, 25-27.

Remaining is the question of the rate and energy distribution of nucleons injected during coalescence in a heavy ion reaction, namely, the source term of Eq. 2. How to calculate and model this is a very interesting and still very open question. In the limit of a light projectile on a heavy target, we might expect a random energy conserving distribution, where the projectile nucleons A_p partition the total energy; we may assume that the many possible couplings of beam velocity and Fermi velocity will cause a randomized sharing of this energy, e.g. that every partition occurs with equal a-priori probability (as given, e.g., by Eq. 3 of Ref. 27). We will do this, and then test the assumption against as broad a range of appropriate heavy ion data as possible. This assumption worked well for light ion induced reactions such as (α,p),[28,29] and we will see if it has some merit for heavy ion reactions as well.

Cindro and his collaborators have made many fine contributions in this regard by finding the best "exciton number" parameter to describe a wide range of heavy ion induced reactions.[30] This work is important for understanding the detailed dependence of the exciton energy distributions on, e.g. angular momentum and impact parameter, and perhaps on injection energy. Scobel and co-workers are currently working on putting this physics directly into the BME.[31]

For the present, we take a less detailed look at our assumption and see if, within the experimental uncertainties, it allows us to

globally reproduce nucleon spectra from central collisions. If we have a reasonable representation of the initial nucleon energy distribution, we may use the model to see if this distribution, and by implication the N-N collision process, in turn causes the other phenomena.

The results of the calculation are not very sensitive to the assumed rate of injection. We assume injection based on the volume of the projectile passing through a plane with a velocity equal to the beam velocity (in the center-of-mass system), reduced appropriately for the Coulomb barrier. We next compare calculated and experimental (HI,n) spectra from several reactions to test the assumptions of our model.

3.0 COMPARISONS OF CALCULATED AND EXPERIMENTAL RESULTS

3.1 HI,n Spectra

In Fig. 3, we show comparisons between evaporation residue (ER) and fission fragment (FF) gated, angle integrated neutron spectra from the ^{20}Ne bombardment of ^{165}Ho, at 11, 15, and 20 MeV/u,[2] and the ER gated neutrons from the ^{12}C + ^{165}Ho reactions at 25 MeV/u.[3] The "experimental results" correspond to angle integrating the fit parameters of the "fast" component. We show calculated results for these spectra using n=20 for ^{20}Ne induced reactions and n=12 for the ^{12}C induced reactions. The value of $n = A_p$ seems to give a satisfactory fit to all the data within uncertainties due to the angle integration method used.

In Fig. 4, we show the ER gated data of Hilscher et al. for ^{20}Ne + ^{165}Ho at 30 MeV/u.[32] The results are shown for integrating the quoted fit parameters and from integrating the data directly over angle. Both sets of results would be reduced by about 18% at the higher energies by transforming into the center-of-mass system, the reference frame in which the calculations are conducted. The BME calculation, using n=20 in the initial exciton distribution, is shown for three values of the nucleon mean free path length : the

nominal value and adjustment of 50% above and below this value. Considering the uncertainties in the angle integration, the calculation using the unadjusted mean free path length gives good agreement with the data. As illustrated in the inset of Fig. 4, our calculation indicates that the high energy neutrons are predominantly emitted in the first ~8×10^{-23} sec.

In Fig. 5, we show a similar comparison for the recent experimental results of Rösch et al.[33] for the reaction $^{40}Ar + ^{40}Ca$ at 20 MeV/u. The data from Ref. 33 were angle integrated directly. The quoted fits to the low temperature ER were used to subtract this component from the resulting total differential multiplicity, leaving the pre-equilibrium component shown in Fig. 5. Our BME calculation uses $\dot{n}=40$ in the initial distribution function, and again the agreement is good. We should emphasize that the absolute values of the calculated spectra are compared with the experimental results in Figs. 3-5 without any normalization, and are calculated without adjustment of the nucleon-nucleon mean free path.

The BME may be seen to give a quite satisfactory agreement for an absolute calculation over a broad range of incident energies and projectiles, yielding spectra correct in shape and magnitude, without normalization of the spectral intensities. We will use the assumption of $n = A_p$ for the remainder of this work, with the caveat that our justification is based only on the comparisons shown in Figs. 3-5. We are, therefore, extrapolating in the absence of centrally-gated experimental data when we treat other systems.

3.2 Comments on Deducing Single Differential Spectra from Double Differential Spectra

Many works have analyzed nucleon spectra resulting from heavy ion reactions with the assumption that the spectra may be represented by several sources, each moving with a constant (fictive) velocity and emitting isotropically in its rest frame. Results of these distributions have been used to deduce precompound decay parameters in heavy ion reactions[2,34,35] and in deducing prefis-

sion, precompound and evaporation neutron multiplicities.[35] In the latter case, additional physical properties were deduced from the results.

We wish to point out that while there is no reason why the constant velocity source argument should be valid for precompound decay, there are good arguments to believe that it should not. First, consider the case in Fig. 6 of a nucleon induced reaction. Experimental results are shown for the ^{209}Bi (p,p') reaction,[36] as well as results calculated with the hybrid precompound decay model.[37] For the latter, we show the contribution from the first term (n=3), for which the incident proton has scattered once with the target nucleons, and for all higher order scattering processes (n>3).

The nucleons emitted following a single scattering event might well give a spectrum characteristic of the nucleon-nucleon center of mass system, i.e., appear to be emitted from a "source" moving at half beam velocity. However, we would expect a different distribution of "source" velocities for nucleons emitted after two or more intranuclear scattering events, or before any nucleon-nucleon collision ("jetting"). The assumption of a single source velocity based on nucleons of high energy would most likely introduce an error in the lower nucleon energies, as Fig. 6 demonstrates that these are the result of multiple scattering. Unfortunately, this is also the region of energy where compound evaporation nucleons may dominate, thereby decreasing sensitivity of the analysis to this problem.

An additional problem in resolution into compound versus precompound components is that an arbitrary mathematical form is assumed to represent the precompound component; one such form used is

$$N(\varepsilon) \propto \varepsilon e^{-\varepsilon/k} \quad . \tag{3}$$

For example, in Ref. 35 for the case of $^{16}O+^{142}Nd$ at 207 MeV beam energy, a value of k=5.5 was deduced for Eq. 3, which was used to extract the precompound neutron multiplicity. Let us proceed by

a different equally arbitrary but more physical approach, instead of assuming the validity of Eq. 3. To do so, we run the Boltzmann Master Equation[27] for an initial exiton number of 16, so that we get emission contributions following all nucleon scattering processes. The results are shown in Fig. 7, compared with the values from Eq. 3, as reported in Ref. 35.

It may be seen that for neutron energies above 12 MeV both approaches are in excellent agreement with each other, and with the experimental results of Gavron et al.[35] (not shown here). However, at lower energies, there is a considerable discrepancy in the predicted multiplicity of precompound neutrons. At the very least, we may conclude that the precompound neutron multiplicity deduced from data is dependent on the method of extraction. An additional example is shown in Fig. 4, where we see different angle integrated spectra resulting from integrating over a moving source parameterization versus an integration performed over the actual experimental results. We must use caution in using the constant source velocity parameterization to integrate experimental spectra or to extract precompound neutron multiplicities. Nuclear model codes may be useful in estimating uncertainties when this is done. It should be recognized that both the constant velocity assumption and the acceptance of Eq. 3 are likely to be in error, and the uncertainties due to these errors should be considered when physical parameters are deduced from results of such analyses.

3.3 Production of High Energy γ-rays

3.3.1 Energy Distributions

The BME may be modified for γ-ray production by addition of the rate for inelastic NNγ scattering,[19]

$$\omega^{pn\gamma}_{ij\to klm} = \frac{\sigma^{klm}_{\gamma pn}(\epsilon_i+\epsilon_j)[2/m)(\epsilon^n_i+\epsilon^p_j)]^{1/2}}{V \sum_{no} g_n g_o \delta(\epsilon^n_i+\epsilon^p_j-\epsilon^n_k-\epsilon^p_l-\epsilon^\gamma_m)} \qquad (4)$$

We need not consider nnγ or ppγ rates, because these quadrupole cross sections are expected to be much smaller than the pnγ dipole cross section.[38] This rate, given in Eq. 4, is entered into the BME (Eq. 2) and we sum over all np collisions to give the total rate of production of γ-rays of energy m:

$$\frac{dN_m}{dt} = \sum_{i+j=min}^{max} \omega_{ij\to klm}^{pn\gamma} \left[n_i^n g_i^n n_j^p g_j^p \;\; g_k^n g_l^p (1-n_k^n)(1-n_l^p) \right] \qquad (5)$$

Implicit in this approach is the assumption that γ-ray emission does not alter the nucleon-nucleon cascade of the relaxation process. To establish $\sigma_{\gamma pn}$, we use a semi-classical radiation formula with two modifications for the γ-ray yield per np collision [19,39,40]

$$\frac{d^2N}{dE_\gamma d\Omega_\gamma} = \frac{1}{E_\gamma} \frac{\alpha}{(2\pi)^2} \sum_{k=1}^{2} \left| \frac{\hat{\varepsilon}_k \cdot \vec{\beta}_i}{1-\hat{q}\cdot\vec{\beta}_i} - \frac{\hat{\varepsilon}_k \cdot \vec{\beta}_f}{1-\hat{q}\cdot\vec{\beta}_f} \right|^2 P_{fac}(1+X) \quad . \qquad (6)$$

In Eq. 6, $\alpha = 1/137$ is the fine structure constant, $\vec{\beta}_i$ and $\vec{\beta}_f$ are the initial and final proton velocities (in units of c) and $\hat{\varepsilon}_1$, $\hat{\varepsilon}_2$ and q are the unit vectors for the two directions of polarization and the γ-ray propagation direction. The modifications to the semi-classical formula are given in the last two factors. Of these $P_{fac} = \beta_f\gamma_f/\beta_i\gamma_i$ is a final state phase space correction.[40] The (1+X) factor allows the magnitude of Eq. 6 to be varied. It was suggested by Brown and Franklin[38] that failure of Eq. 6 to include meson exchange processes should require $X \sim 1$ as a correction. This approximation is tested in Fig. 8 against the p+d→γ spectrum of Edgington and Rose,[41] measured with 140 MeV protons. Because $pp\gamma \ll pn\gamma$,[38] the deuteron target approximates a neutron target with some Fermi motion. In Fig. 8, we see the result of Eq. 6 with X=0, but averaged over the target neutron Fermi motion,[42] and we also show the result using X=1. The agreement with the latter is quite satisfactory, so we use X=1 for the remainder of this work.

Neuheuser and Koonin have recently evaluated the quantum mechanical analog of Eq. 6.[43] We show their result in Fig. 8 also. Because the agreement with the d(p,γ) spectrum is poor we do not adopt this result; we will, however, show results of this formulation in several figures. A weakness of our reliance on Eq. 6 with X=1 is that we have compared only with the 140 MeV d(p,γ) spectral data of Ref. 41. Clearly similar experimental spectra at other incident proton energies would be extremely valuable to confirm our reliance on Eq. 6 with X=1.

We further test Eq. 6 by using it with Eqs. 4 and 5 in the BME for the $^{12}C(p,\gamma)$ and Pb(p,γ) inclusive spectra[41] also shown in Fig. 8. The agreement, with no normalization (having accepted X = 1 in Eq. 6) is excellent. Next, we perform the calculation for nucleus-nucleus data sets, using all published results of which we were aware. These results are presented in Figs. 9-13.

In Fig. 9, we show the results of Stevenson et al.,[8] whose detection system consisted of a stack of lucite as Cerenkov detectors. The agreement of calculated spectra, with no parameter variation, is satisfactory. The quantal result[43] gives spectra which are a little high. Recent detector calibrations suggest that the results of Ref. 8 should be increased twofold.[44] If this is so, we would get better agreement using a larger reaction cross section than given by the $\sigma_R=\pi r_o^2 A_T^{2/3}$ assumed for all γ-ray calculations presented herein. In Figs. 10 and 11, we see results of Kwato, Njock et al.[9] and Bertholet et al.[10] using ^{40}Ar and ^{86}Kr projectiles at 30 and 44 MeV/u, respectively. The ^{86}Kr data represent an extrapolation of the assumptions on initial nucleon distributions based on results shown in Figs. 3-5. Nonetheless, we find excellent agreement between calculated and experimental results. These data were measured with a stack of plastic scintillators followed by a NaI detector. In Fig. 12, we show results of Alamanos et al. for 35 MeV/u ^{14}N reactions on Ni nuclei[11] measured with lead glass detectors; our calculation fails to reproduce these data satisfactorily.

In Fig. 13, we show the results of Grosse et al[12,13] for 48-84 MeV/u ^{12}C projectiles on ^{12}C and ^{238}U targets. Again, our calculation seriously underestimates the data. The quantal result, on the other hand, is in satisfactory agreement with these data. Lead glass detectors were used in measuring the data in Fig. 13.

IV. CONCLUSIONS

The BME model is transparent in the physics used to treat the equilibration process, specifically, a series of N-N collisions whose rate is determined by free scattering cross sections moderated by the Pauli exclusion principle. The BME is very versatile and it is easy to use to test ideas; e.g., pion production cross-sections, incomplete momentum transfer. The model works well in reproducing nucleon emission spectra for central collision processes using an input distribution based on $n = A_p$. More work needs to be done in modeling the initial nucleon distribution function with consideration of the coupling constraints, phase space constraints, and with angular momentum averaging.

A broader range (projectile and projectile energy variations) of nucleon and cluster emission spectra gated on central collisions would be welcome as a more severe test of the BME and other precompound decay models. Measurement of nucleons at the highest kinetic energies may give crucial information on the microscopic details of the coalescence process, in particular the coupling of relative motion and Fermi motion of the projectile nucleons, and of the viability of the N-N collision process for subthreshold pion production.

All caveats considered, simple precompound decay models yield a wealth of insight into the dynamics of heavy ion reactions. Many of the predictions, made as early as 1974 by use of these models,[16,45] are now being realized in experimental measurements. These models should continue to be strong tools in the interpretation of heavy ion reactions. We have shown that all the phenomena analyzed in this work may be interpreted in terms of a N-N collision mechanism,

getting excellent agreement with nearly all data without parameter variation. Similar tests of other models and theories would be useful to narrow the choice of viable interpretations.

References

1. T. C. Awes et al., Phys. Rev. C 25, 2361 (1982).

2. E. Holub et al., Phys. Rev. C 28, 252 (1983).

3. E. Holub et al., Phys. Rev. C 33, 143 (1986).

4. T. Johansson et al., Phys. Rev. Lett. 48, 732 (1982); H. Noll et al., Phys. Rev. Lett. 52, 1284 (1984).

5. J. Stachel et al., in Proceedings of the Institute for Nuclear Studies, RIKEN Symposium on Heavy Ion Physics, Tokyo, Japan (1984) unpublished.

6. H. Heckwolf et al., Z. Phys. A 315, 243 (1984).

7. G. R. Young et al., Phys. Rev. C 33, 742 (1986).

8. J. Stevenson et al., Phys. Rev. Lett. 57, 555 (1986).

9. M. Kwato Njock et al., Phys. Lett. B175, 125 (1986).

10. R. Bertholet et al., Journal de Physique, Colloque C4, supplement au no 8, Tome 47, aout (1986); H. Nifenecker et al., XXIV Int'l. Winter Meeting on Nucl. Phys., Bormio, Italy (1986).

11. N. Alamanos et al., Phys. Lett. B174, 392 (1986).

12. E. Grosse et al., Europhys. Lett. 2, 9 (1986).

13. E. Grosse, from talk given at the International Workshop on Gross Properties of Nuclei, Hirschegg (1985).

14. H. Nifenecker, private communication (1987).

15. D. Vasak, H. Stöcker, B. Müller and W. Greiner, Phys. Lett. 93B, 243 (1980), and D. Vasak, B. Müller and W. Greiner, Physica Scripta 22, 25 (1980); D. Vasak, W. Greiner, B. Müller, T. Stahl and M. Uhlig, Nucl. Phys. A428, 291c (1984); D. Vasak, B. Müller and W. Greiner, J. Phys. G11, 1309 (1985); R. Heuer, B. Müller, H. Stöcker and W. Greiner, Institut für Theoretische Physik, Johann Wolfgang Goeth Universität preprint no. UFTP-204 (1987).

16. M. Blann, A. Mignerey and W. Scobel, Nukleonika 21, 335 (1976); M. Blann, Phys. Rev. C 23, 205 (1981).

17. M. Blann, Phys. Rev. C 31, 295 (1985).

18 M. Blann, Phys. Rev. C 32, 1231 (1985); Phys. Rev. Lett. 20, 2215 (1985).

19. B. A. Remington, M. Blann and G. F. Bertsch, Phys. Rev. Lett. 57, 2909 (1986); B. A. Remington, M. Blann and G. F. Bertsch, Phys. Rev. C35, 1720 (1987); B. A. Remington and M. Blann, Phys. Rev. C36, 1387 (1987).

20. G. Bertsch, in "Frontiers in Nuclear Dynamics," ed. by R. A. Broglia and C. H. Dasso (Plenum Press, 1985), p. 277.

21. J. Aichelin, Phys. Rev. C 33, 537 (1986).

22. J. J. Molitoris and H. Stöcker, Phys. Rev. C 32, 346 (1985).

23. W. Cassing, T. Biro, U. Mosel, M. Tohyama, and W. Bauer, Phys. Lett. B181, 217 (1986).

24. W. Bauer, G. F. Bertsch, W. Cassing, U. Mosel, Phys. Rev. C 34, 2127 (1986).

25. G. D. Harp, J. M. Miller and B. J. Berne, Phys. Rev. 165, 1166 (1968).

26. G. D. Harp and J. M. Miller, Phys. Rev. C 3, 1847 (1971).

27. M. Blann, Phys. Rev. C 31, 1245 (1985).

28 M. Blann, Ann. Rev., Nucl. Sci. 25, 123 (1975).

29. J. Bisplinghoff and H. Keuser, Phys. Rev. C 35, 821 (1987).

30. N. Cindro, M. Korolija and E. Holub, "Fundamental Problems in Heavy ion Collisions, " ed. by N. Cindro, et al., p. 301, World Scientific, Singapore (1985).

31. W. Scobel, private communication (1986).

32. D. Hilscher et al., Phys. Rev. C 36, 208 (1987).

33. W. Rösch et al., Phys. Lett. B197, 19(1987).

34. D. Hilscher, E. Holub, U. Jahnke, H. Orf and H. Rossner in "Proceedings of the Third Adriatic Europhysics Study Conference," Hvar, Yugoslavia (1981) Ed. N. Cindro, R. A. Ricci and W. Greiner (North Holland, Amsterdam 1981) p. 225.

35. A. Gavron et al., Phys. Rev. C 35, 579 (1987).

36. F. E. Bertrand and R. W. Peelle, Phys. Rev. C 8, 1045 (1973).

37. M. Blann, Ann. Rev. Nucl. Sci. 25, 123 (1975).

38. V. R. Brown, Phys. Rev. 177, 1498 (1969); V. R. Brown and J. Franklin, Phys. Rev. C 8, 1706 (1973); K. W. Rothe, P. F. M. Koehler, and E. H. Thorndike, Phys. Rev. 157, 1247 (1967).

39. J. D. Jackson, Classical Electrodynamics, (Wiley, New York, 1975), p. 703.

40. Che Ming Ko, G. Bertsch and J. Aichelin, Phys. Rev. C 31, 2324 (1985); K. Nakayama and G. Bertsch, Phys. Rev. C 34, 2190 (1986).

41. J. A. Edgington and B. Rose, Nucl. Phys. 89, 523 (1966).

42. C. Ciofi degli Atti, E. Pace and G. Salme, Phys. Lett. B 141, 14 (1984).

43. D. Neuhauser and S. E. Koonin, Nucl. Phys. A 462, 163 (1987).

44. J. Stevenson, private communication (1987).

45. M. Blann, Nucl. Phys. A 235, 211 (1974); M. Blann, Proceedings of the International School on Nuclear Physics, Predeal, Romania 1974, ed. A. Ciocanel, p. 249, Bucharest (1976).

This work was performed under the auspices of the U.S. Department of Energy by the Lawrence Livermore National Laboratory under contract number W-7405-ENG-48.

1300A-12/2/87

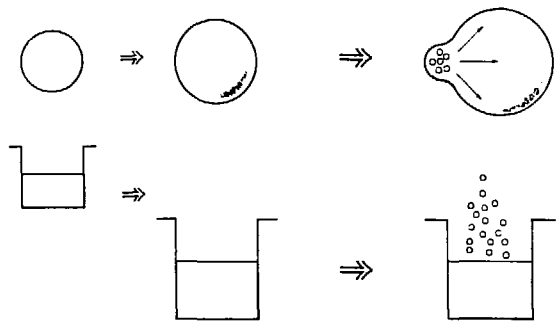

1) Diagrammatic representation of a heavy ion collision in geometric (upper) and energy (lower) space. This figure is described in the text.

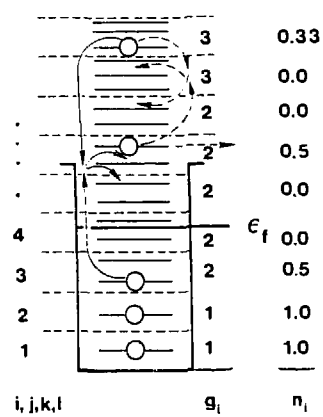

2) Representation of a Fermi gas nucleus as treated in the Boltzmann Master Equation. The nucleus is divided into 1 MeV wide energy bins, indexed by i, j, k or l, counting from the bottom of the Fermi sea.

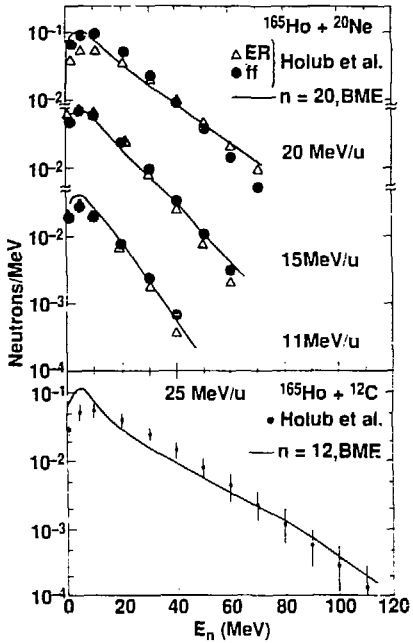

3) Calculated and experimentally deduced spectra for the ^{165}Ho(^{20}Ne,n) and the ^{165}Ho(^{12}C,n) systems at 300 MeV. Experimental points from Refs. 2,3 result from an integration of a moving source fit to experimental yields for the fast component only. Experimental yields for ^{20}Ne projectiles were gated on evaporation residues (ER) as represented by open triangles, and on fission fragments (FF) shown by closed circles. Results for ^{12}C were gated on ER. Calculated results are shown for the BME with n = A_p in the exciton distribution function, where we assume total excitation is shared by n excitons with equal a-priori probability.

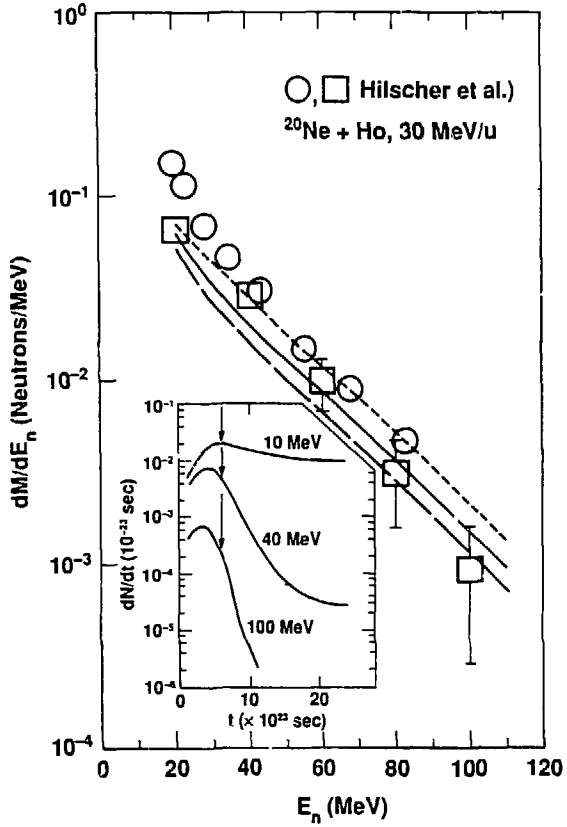

4) Experimental and calculated neutron energy spectra from 30 MeV per nucleon ^{20}Ne on Ho. The squares represent the pre-equilibrium yields deduced by Hilscher et al.[32] by fitting an assumed isotropically emitting moving source to the high energy data. The circles represent the total differential multiplicity, and are the results of angle integrating the double differential data of Hilscher et al. directly. The solid line is the BME result; the short and long dashed lines correspond to increasing and decreasing the mean free path by 50%. The insert shows the calculated time dependence of the emission of 10, 40 and 100 MeV neutrons. The arrows represent the time at which fusion is assumed complete in the calculation.

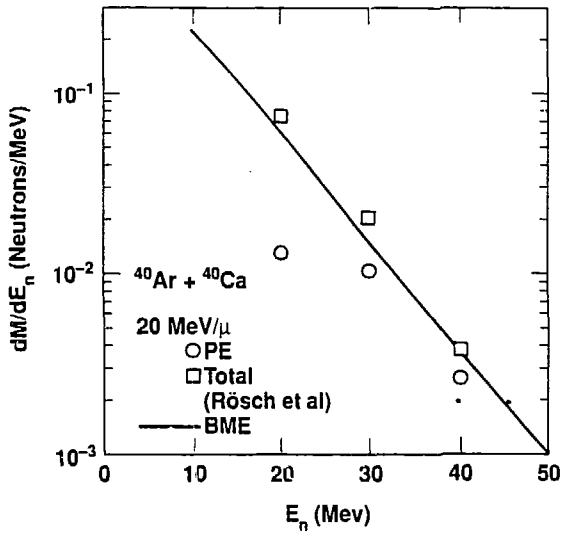

5) Calculated and experimental $^{40}Ca(^{40}Ar,n)$ spectra for 20 MeV/u incident energy, gated on evaporation residues. Data are from Ref. 33. The solid line is the result of the BME calculation assuming 40 excitons.

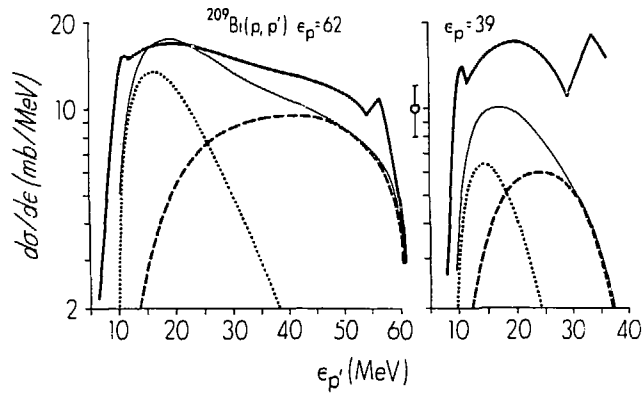

6) Experimental and calculated ^{209}Bi (p,p') spectra for 62 and 39 MeV incident protons. The heavy solid curve is the experimental result of Bertrand and Peelle.[36] The dashed curve is the first term (n=3) of the geometry dependent hybrid model;[37] all higher order terms are included in the dotted curve. The thin solid curve is the sum of all calculated components.

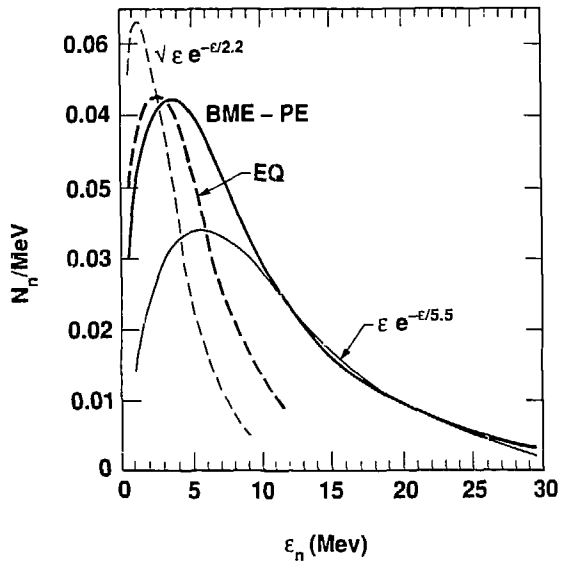

7) Comparison of calculated equilibrium and precompound neutron spectra. The heavy solid curve is the precompound result of the Boltzmann Master Equation with n_0=16; the thin solid curve is the result of Eq. 3 with k=5.5. The heavy dashed curve is the BME equilibrium result; the thin dashed curve is the result of the expression indicated.

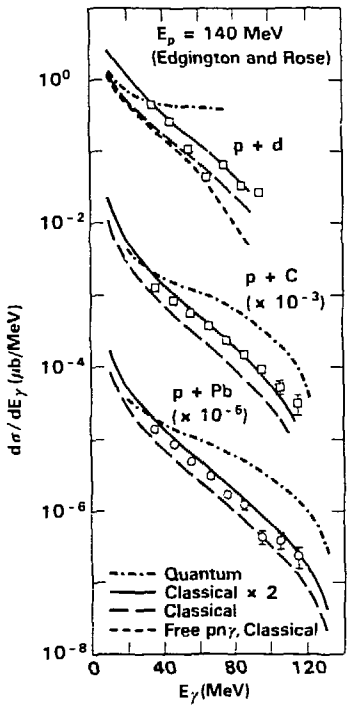

8) Calculated and experimental γ-ray spectra resulting from 140 MeV protons incident on d, C, and Pb targets. Data are from Ref. 41. The short dashed line in the p+d spectrum is the calculation of Eq. 6 for X=0. The long dashed curve is the result of folding over the neutron Fermi motion. The solid line is the result of next setting X=1 in Eq. 6. The open symbols represent data points. The dot-dash curve corresponds to using the calculated npγ bremsstrahlung cross section of Ref. 43, as opposed to that of Eq. 6.

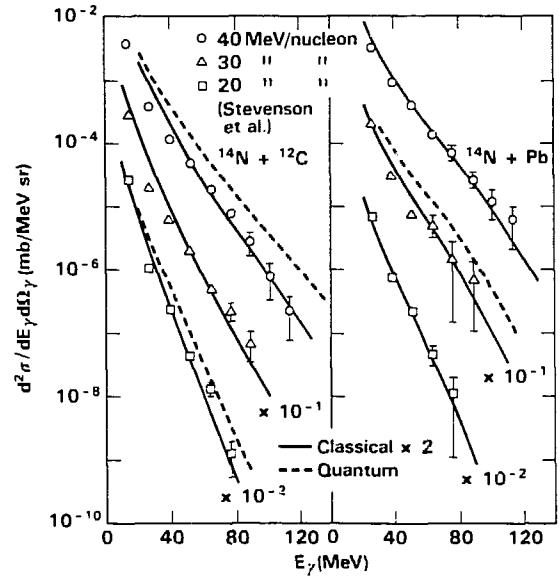

9) Calculated and experimental γ-ray spectra from ^{14}N bombardment of ^{12}C and Pb at 20, 30 and 40 MeV/nucleon. Data are from Ref. 8. The solid lines are the predicted spectra based on using Eq. 6 with X = 1 in the BME. The dashed curves are the result of using the values from Ref. 43.

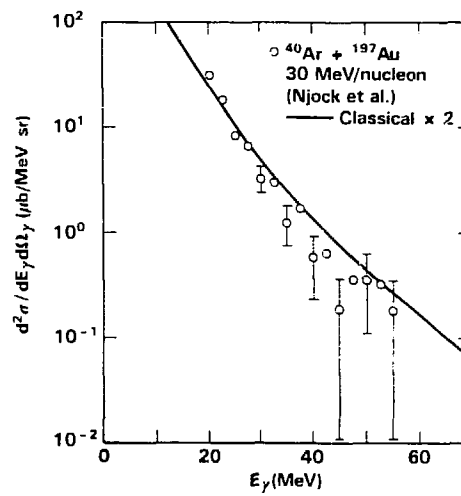

10) Results of the BME calculation compared with experimental γ-ray spectra for 30 MeV/u ^{40}Ar on ^{197}Au. Data are from Ref. 9. Calculation uses Eq. 6 with X = 1, denoted "classical X 2."

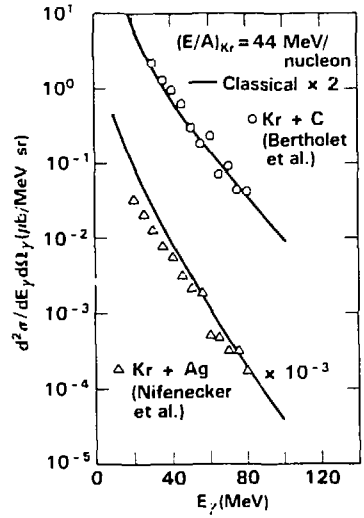

11) Calculated (BME) and experimental γ-ray spectra from 44 MeV/u Kr on C and Ag targets. Experimental results are from Ref. 10.

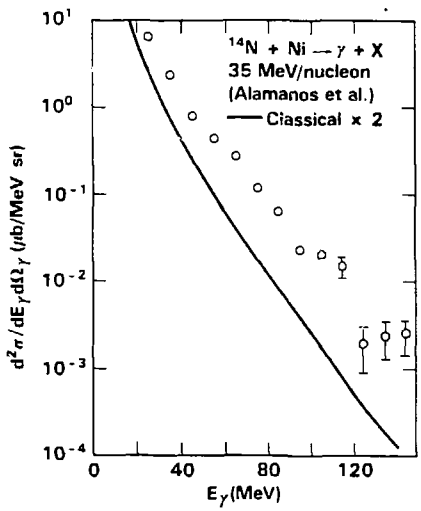

12) Calculatd (BME) and experimental γ-ray spectra from 35 MeV/u ^{14}N + Ni. Data are from Ref. 11.

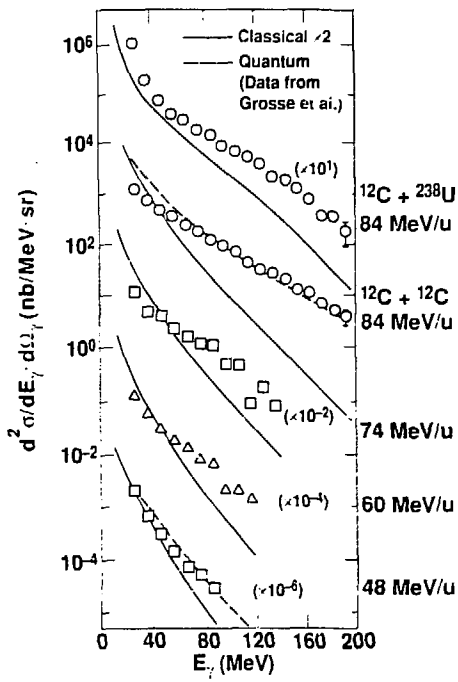

13) Calculated and experimental γ-ray spectra for ^{12}C bombardment of ^{238}U at 84 MeV/u (top set), and on ^{12}C targets at 84, 74, 60 and 48 MeV/u, as indicated. Data are from Refs. 12 and 13. The dashed line show the results of a BME calculation using the calculated NNγ bremsstrahlung cross sections from Ref. 43 rather than those calculated from Eq. 6.